J Mater Sci (2010) 45:4884–4888
DOI 10.1007/s10853-010-4665-3

ULTRAFINE GRAINED MATERIALS

Fabrication and oxidation resistance of nanocrystalline Fe10Cr alloy

Rajeev K. Gupta · R. K. Singh Raman · Carl C. Koch

Received: 17 February 2010 / Accepted: 26 May 2010 / Published online: 9 June 2010

Abstract Nanocrystalline (*nc*) and microcrystalline (*mc*) Fe10Cr alloys were prepared by high energy ball-milling followed by compaction and sintering, and then oxidized in air for 52 h at 400 °C. The oxidation resistance of *nc* Fe10Cr alloy as determined by measuring the weight gain after regular time intervals was compared with that of the *mc* alloy of same chemical composition (also prepared by the same fabrication route and oxidized under identical conditions). Oxidation resistance of *nc* Fe10Cr alloy was found to be in excess of an order of magnitude superior than that of *mc* Fe10Cr alloy. This article also presents results of secondary ion mass spectrometry (SIMS) of oxidized samples of *nc* and *mc* Fe–Cr alloys, evidencing the formation of a more protective oxide scale in the *nc* alloy.

Introduction

Synthesis of nanocrystalline Fe–Cr alloys

Nanocrystalline (*nc*) alloys have been produced by processes such as ball-milling, sputtering, electron beam evaporation, pulse laser ablation [1], gas condensation [2, 3], and sol–gel [4] method. Among these techniques, high energy ball-milling has been most widely used because of simplicity and potential to scale up for large production [5–7]. However, ball-milled powders require to be compacted. Groza [8] has reviewed various techniques employed for compaction of different *nc* materials, viz., high pressure/lower temperature compaction, in situ consolidation [9], hot compaction [10], hot iso-static pressing [11], explosive compaction [12]. However, compaction of *nc* Fe–Cr alloys appears to be a non-trivial task. The difficulties arise due to the restrictions on plastic deformation posed by the high hardness, which necessitates high pressures/temperatures for consolidation and sintering, for example, pure iron with an average grain size of 10 nm shows a hardness value of 10 GPa [13]. Plastic deformation, which is a necessary condition for effective compaction requires applied pressure to be in excess of yield stress and approximately one-third of the hardness (i.e., 3.5 GPa), for which facilities are not easily available in most research laboratories. Plastic flow, high densification, and inter-particle bonding can be achieved by compaction/sintering at high temperatures. However, fabrication at excessively high temperatures will lead to the common instances of grain growth.

It may be possible to produce *nc* Fe–Cr alloys with close to theoretical density and without too excessive grain growth, by employing a suitable combination of temperature and pressure in hot compaction process. The other possibility could be, to soften the material, by prior thermal treatment. The latter may be less effective but, attractive for the situations where hot compaction facilities are not readily available. This article presents a description of the success in exploring the suitable fabrication window for *nc* Fe–Cr alloys, for circumventing the fabrication hurdles, as described earlier.

R. K. Gupta (✉) · R. K. Singh Raman
Department of Mechanical and Aerospace Engineering, Monash University, Melbourne, VIC 3800, Australia
e-mail: Rajeev.Gupta@eng.monash.edu.au

R. K. Singh Raman
Department of Chemical Engineering, Monash University, Melbourne, VIC 3800, Australia

C. C. Koch
Department of Materials Science and Engineering, North Carolina State University, Raleigh, NC 27695-7907, USA

Oxidation resistance of nanocrystalline alloys

Nanocrystalline materials are characterized by a grain size of up to about 100 nm whereas submicron materials are characterize by a grain size of up to 0.1–0.3 μm [1, 2]. When the grain size is below a critical value (5 nm), more than 50 vol% of atoms are associated with the grain boundaries. Consequently, properties of the *nc* materials differ significantly as compared to conventional microcrystalline (*mc*) materials of similar chemical compositions [1, 2, 14]. The structure, high grain boundary area fraction, change in thermodynamic properties, and diffusion of impurities and alloying elements can cause considerable differences in oxidation behavior of *nc* materials [1, 2, 15–18].

It was believed that *nc* metals and alloys may have inferior oxidation resistance due to their large volume fraction of grain boundaries and triple points. On the contrary, many investigations have reported enhanced oxidation resistance due to *nc* structure. For instance, oxidation resistance of FeBSi [19], Ni-based alloys [20], Zr and its alloys [21], Cr-33Nb [22], and Cu–Ni–Cr alloys [23] is reported to be superior in their *nc* form. It is noted that the improved oxidation resistance in *nc* alloys arises mainly because of the faster diffusion of elements that can form passive oxide film and/or because of improved adhesion of passive film formed over *nc* structure.

A number of studies have examined the oxidation resistance of conventional microcrystalline Fe–Cr alloys, and it is established that formation of Cr oxide layer in higher Cr alloys and Fe–Cr mixed oxide layer in relatively low-Cr alloys (which largely depends on the diffusion of Cr from bulk to the alloy/oxide interface) is the governing mechanism of oxidation resistance of Fe–Cr alloys [24–27]. It has already been shown that grain refinement in Fe–Cr and Ni–Cr alloys improves their oxidation resistance because of faster diffusion of Cr caused by increased fraction of grain boundaries [24, 27–31]. However, grain refinement in most of the investigations is limited to the micrometric regime.

Diffusion of alloying elements and impurities in *nc* alloys is reported to be several orders of magnitude greater than that in their microcrystalline counterparts. Therefore, Fe–Cr alloys where diffusion of Cr plays major role in determination of oxidation resistance, *nc* structure may facilitate the establishment of Cr oxide layer and as a result, the necessary oxidation resistance may be attained at much lower Cr contents (than in the case of microcrystalline alloys of same composition).

This study presents a comparison of oxidation resistance of *nc* and microcrystalline Fe10Cr alloys at 400 °C.

Experimental procedure

Synthesis of nanocrystalline Fe–Cr alloys

Fe–Cr alloy with a nominal Cr content of 10 wt% was prepared by mechanical alloying (using a SPEX model 8000 shaker mill). As starting materials, high purity powders (99.9% purity and particle size <10 μm) of Fe were loaded into a tool steel vial under vacuum with 440C stainless steel balls (6.4–7.9 mm in diameter). Ball-to-powder weight ratio was kept at 10:1. High energy ball-milling was carried out for 20 h. Ball-milled *nc* alloy powder was annealed at 500, 600, and 700 °C in forming gas atmosphere (98% Ar + 2% H_2) in order to understand the grain growth kinetics.

On the basis of the grain growth data, the ball-milled alloy powders were annealed at 600 °C in a forming gas atmosphere for 30 min. Ball-milled and annealed powders were compacted at room temperature into pellets (diameter = 12 mm and thickness = 1.5 mm) under a uni-axial pressure of 3GPa. Density of the pellets (before and after sintering) was measured by gas pyconometry. The compacted pellets were sintered at 600 °C for 1 h in forming gas atmosphere to improve the density and interparticle bonding.

X-ray diffraction (XRD) was performed on the as-milled, annealed, and compacted samples with a CuK_α radiation ($\lambda = 0.1541$ nm) at a scan rate of 0.3°/min, and at 50 steps per degree. Grain size of the *nc* alloy after various stages of fabrication was determined from the X-ray peak broadening using the Voigt function [32], after eliminating the instrumental and lattice strain contributions to peak broadening. The four most intense peaks (110, 200, 211, 220) were used to calculate the grain size. In order to ensure reproducibility, several annealing treatments and the X-ray analyses were duplicated. The accuracy of the grain size determination was within ±4 nm.

Oxidation resistance of *nc* vis-a-vis microcrystalline Fe–Cr alloys

The compacted and sintered disks of *nc* and microcrystalline Fe10Cr alloys were polished to 2400 grit silica paper finish and subjected to oxidation in air for durations up to 3120 min (52 h) at 400 °C. At this temperature the grain boundary diffusion is much greater than the lattice diffusion. For the particular investigation of the role of nanometric vis-à-vis micrometric grain size in the development of oxidation resistance, a *mc* Fe-10 wt% Cr alloy with much larger grain size (1.5 μm) was simultaneously subjected to the same oxidation treatment as the *nc* Fe–Cr alloy. Weight change during the oxidation was recorded by

weighing the samples in a Cahn balance (least count 0.1 mg) after regular time intervals. Weight gain experiments were repeated several times to ensure the reproducibility of the results.

In order to understand the role of the nanostructure on oxidation rate, thin oxide films formed during oxidation need to be characterized for the Cr content. Cr content of oxide layers on Fe–Cr alloys have earlier been characterized by secondary ion mass spectrometry (SIMS) [33–35]. The thin oxide films formed in different durations at 400 °C over *nc* and microcrystalline Fe-10 wt% Cr alloys were characterized by SIMS depth profiling, using a Cameca ims (5f) dynamic SIMS instrument. Other SIMS parameters were: Cs^+ ion primary beam (10 nA), depth profiling of craters of 250 μm × 250 μm area. In dynamic SIMS instrument, Cs^+ ions were used to sputter the oxide film and elemental analysis was performed simultaneously to characterize the composition of the oxide film.

Results and discussion

Synthesis of nanocrystalline and microcrystalline materials

Grain growth behavior of the ball-milled *nc* Fe10Cr alloy at 500, 600, and 700 °C is presented in the Fig. 1. Grain size after various steps of annealing was determined using XRD analysis as described in "Synthesis of nanocrystalline Fe–Cr alloys" section. As evident from the Fig. 1, initial grain growth is rapid at each of the three temperatures and is a strong function of temperature, as suggested from the increasing intensity of the initial grain growth with temperature (Fig. 1). Annealing at 500 °C marks a rapid grain growth in the beginning which was limited to the first 15 min, and no significant change in grain size in the course of further annealing. At 600 and 700 °C, grains continued to grow with time, even beyond 15 min.

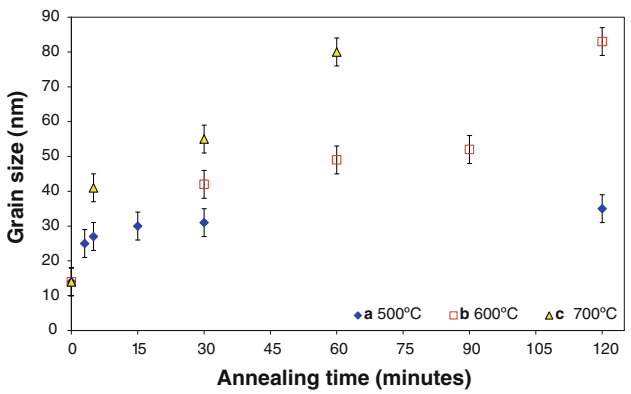

Fig. 1 Grain growth of Fe10Cr alloy at: (*a*) 500 °C, (*b*) 600 °C and (*c*) 700 °C

Compaction of the ball-milled powder under a uni-axial pressure of 3 GPa at room temperature was not successful, as this resulted in disintegration of the pellets. It became obvious that it would be necessary to reduce hardness and improve ductility of the powder, before it was subjected to the pressure compaction. Based on the grain growth data shown in Fig. 1, a prior annealing at 600 °C for 30 min was selected with a view to prior softening of the powder without any excessive grain growth. Prior annealing at 600 °C for 30 min though resulted in some grain growth (Fig. 1), the grain size of the alloy was still found to be well within the *nc* range (42 nm). Most importantly, because of the softening caused by the prior annealing, it was possible to compact the powder into pellets (diameter = 12 mm, thickness = 1.5 mm) at a pressure of 3 GPa at the room temperature. As a result of this compaction, the green density of the material obtained was close to the theoretical density. Compacted pellets were sintered for 1 h at 600 °C, which further improved the density close to 100% of the theoretical density. However, the sintering caused some further grain growth. The grain size of the sintered pellets was determined to be 52 nm (±4 nm).

To prepare microcrystalline alloy specimens, ball-milled powders of Fe10Cr alloy were annealed at 600 °C then compacted under a uniaxial pressure of 3 GPa and then sintered at 840 °C for 3 h. Test specimen of both *nc* and microcrystalline Fe10Cr alloys were 12 mm in diameter and 1.5 mm in thickness. Grain size of microcrystalline material as determined by optical microscopy was 1.5 μm. Density and grain size of the samples (used in the current study) after various processing steps are presented in Table 1.

Oxidation of nanocrystalline and microcrystalline Fe-10% Cr alloys

In order to compare the influence of *nc* and *mc* structures on oxidation of Fe10Cr alloy, the compacted and sintered pellets of both *nc* and microcrystalline Fe10Cr alloys were oxidized at 400 °C for durations up to 3120 min. Oxidation kinetics data (Fig. 2) show the microcrystalline alloy to be oxidizing at a considerably greater rate than the *nc* alloy. After 3120 min of oxidation, weight gain of microcrystalline Fe10Cr alloy was found to be nearly 18 times greater than that of the *nc* Fe10Cr alloy.

As described in "Oxidation resistance of nanocrystalline alloys" section above, oxidation resistance of Fe–Cr alloys is associated primarily to the chemical characteristics and the Cr content of the thin inner oxide scale. Oxide layer with greater Cr content provides superior oxidation resistance. Availability of sufficient Cr at the alloy–oxide

Table 1 Grain size and density of the test specimens after various fabrication steps

	Grain size, ball-milled powder	Annealing, ball-milled powder	Grain size, ball-milled and annealed powder	Green density, compacted pellets (% of theoretical density)	Sintering compacted pellets	Density, sintered pellets (% of theoretical density)	Grain size, sintered pellets (test specimen)
nc Fe10Cr	14 nm	600 °C/30 min	42 nm	~100	600 °C/60 min	~100	52 nm
mc Fe10Cr	14 nm	600 °C/30 min	42 nm	~100	840 °C/180 min	~100	1.5 μm

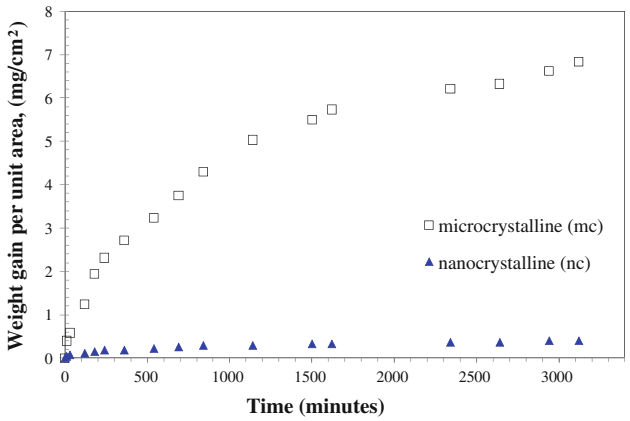

Fig. 2 Oxidation kinetics of nanocrystalline (*nc*) and microcrystalline (*mc*) Fe10Cr alloys oxidized at 400 °C for 3120 min

interface is essential for the effectiveness of internal to external oxidation transition to form a continuous Cr_2O_3 layer. Establishment of such continuous oxide layer of solute depends on the several factors which include: (a) the concentration and diffusion of the solute in the alloy, (b) the diffusion of the oxygen in the alloy, (c) diffusion of oxygen in the external oxide film, and (d) the growth rate of the solute-oxide layer. In practice this means that, under a particular set of conditions, continuous and protective scale of solute-oxide forms at or above a critical concentration of solute (B, in a binary alloy A–B) which has been given as per following equation [29, 36, 37]:

$$N_B = \frac{V}{z_B M_o}\left(\frac{\pi k_p}{D_B}\right)^{\frac{1}{2}}$$

where N_B is the critical amount of solute B required for the formation of an external solute-oxide layer, V is the molar volume of the alloy, Z_B is the valance of the B atoms, M_O is the atomic weight of oxygen, D_B is the diffusion coefficient of B in the alloy, and k_p is the parabolic rate constant for the exclusive formation of the B-oxide (B can be substituted by Cr in the case of Fe–Cr system).

At a given temperature and external oxygen partial pressure, the critical amount of Cr required for the formation of external Cr_2O_3 layer will only depend upon the diffusion coefficient of Cr in the alloy. Diffusivity of the alloying elements in *nc* materials is reported to be much greater than that in microcrystalline materials [17, 18]. Diffusion in a material can be characterized as the combined effect of diffusion through the grain boundaries and lattice diffusion and can be written as:

$$D = f\left(D_{gb}\right) + (1-f)D_b$$

where f is the grain boundary area fraction, D_{gb} is the grain boundary diffusion coefficient, and D_b is the bulk diffusion coefficient. The grain boundary area fraction (in *nc* materials) is much greater than that in microcrystalline materials and therefore contribution of grain boundary diffusion coefficient in *nc* materials is significantly greater which leads to a significant increase in the overall diffusion coefficient of alloying elements.

Since the diffusivity of Cr in the *nc* alloys is a few orders of magnitude greater [17, 18], the critical amount of Cr required for the formation of an external Cr_2O_3 scale drops down significantly and considerable oxidation resistance is obtained at lesser Cr contents. On the other hand, diffusivity of Cr in microcrystalline Fe10Cr alloy is several orders of magnitude lower, and hence 10% Cr is not enough to form an external Cr_2O_3, which explains the considerably greater weight gains of the microcrystalline alloy at 400 °C.

The considerable difference in the Cr enrichment in the inner oxide scale developed on the *nc* and microcrystalline alloys has duly been correlated by SIMS depth profiles (Fig. 3). The most notable finding of the SIMS profiles is that the highest Cr content of the inner layer of *nc* Fe10Cr alloy is considerably greater than the highest Cr content in the inner layer of microcrystalline Fe10Cr alloy. At this considerably higher Cr content of the oxide layer on *nc* Fe10Cr alloy, the inner oxide layer can be assumed to be of Cr_2O_3, which will establish that it is possible to develop a protective layer of Cr_2O_3 in the case of *nc* Fe–Cr alloys at considerably low Cr contents and therefore it is possible to form a Cr_2O_3 scale in *nc* Fe10Cr alloy. As the reported literature [33–35] would suggest, inner oxide layer of the microcrystalline alloys with low Cr (<12%) would at best be a mixed spinel type Fe–Cr oxide. Such low Cr alloys would fail to develop a Cr_2O_3 layer. It seems the considerably greater oxidation rate of microcrystalline Fe10Cr alloy (as compared to *nc* Fe10Cr alloy) can be explained on the basis of the considerably higher Cr content of the inner oxide layer and possible development of the protective oxide layer of Cr_2O_3 over the latter.

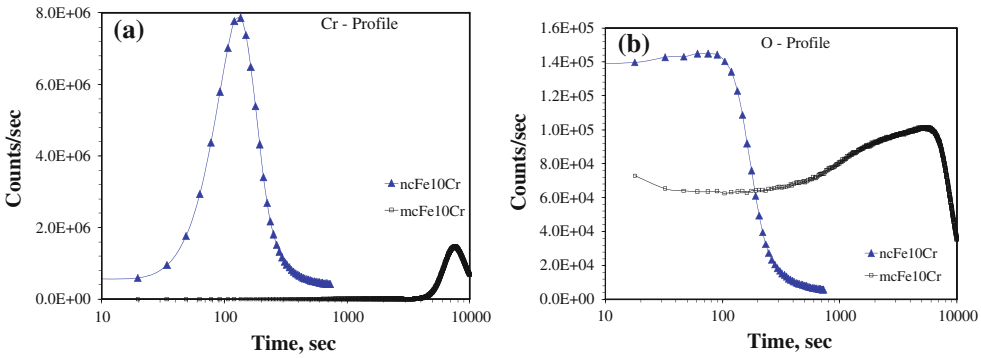

Fig. 3 SIMS depth profiles of **a** Cr and **b** O in the oxide scales developed on nanocrystalline (*nc*) and microcrystalline (*mc*) Fe-10% Cr alloys during oxidation at 400 °C for 3120 min

Conclusions

1. It has been possible to produce *nc* Fe-10% Cr alloy by ball-milling route. Though hot compaction would be an ideal choice, the alloy powder could be successfully compacted close to the theoretical density, by employing a step of prior annealing of the powder. The compacted pellets have been successfully sintered while retaining the grain size within the *nc* range.
2. Oxidation resistance of *nc* Fe10Cr alloy is found to be far better than that of microcrystalline alloy of similar chemical composition. SIMS depth profiling and theoretical understanding of oxidation of Fe–Cr alloy further verify that the improved oxidation resistance of *nc* alloys is due to the formation of a Cr-rich oxide layer.

Acknowledgements The authors acknowledge support of Australian Research Council (ARC) with a grant (DP0665112) to carry out this study, under their Discovery grant scheme. The authors are also thankful to the support of Australian Institute of Nuclear Science and Engineering (AINSE) for carrying out the SIMS work.

References

1. Koch CC, Youssef KM, Scattergood RO, Murty KL (2005) Adv Eng Mater 7:787
2. Gleiter H (1989) Prog Mater Sci 33:223
3. Trapp S, Limbach CT, Gonser U, Campbell SJ, Gleiter H (1995) Phys Rev Lett 75:3760
4. Roy RA, Roy R (1984) Mater Res Bull 19:169
5. Cheng S, Ma E, Wang YM, Kecskes LJ, Youssef KM, Koch CC, Trociewitz UP, Han K (2005) Acta Mater 53:1521
6. Youssef KM, Scattergood RO, Murty KL, Horton JA, Koch CC (2005) Appl Phys Lett 87:1
7. Youssef KM, Scattergood RO, Murty KL, Koch CC (2006) Scripta Mater 54:251
8. Groza JR (2007) In: Koch CC (ed) Nanostrucutued materials: processing, properties and applications. William Andrew Pub, Norwich, NY
9. Youssef KM, Scattergood RO, Murty KL, Koch CC (2004) Appl Phys Lett 85:929
10. Kedim OE, Cao HS, Guay D (2002) J Mater Process Technol 121:383
11. Rawers J, Biancaniello F, Jiggetts R, Fields R, Williams M (1999) Scripta Mater 40:277
12. Guruswamy S, RL M, Srisukhumbowornchai N, Michael KM, Joseph P (2000) IEEE Trans 36:3219
13. Siegel RW (1997) Mater Sci Forum 235–238:851
14. Palumbo G, Thorpe SJ, Aust KT (1990) Scripta Metall Mater 24:2347
15. Zhao YH, Sheng HW, Lu K (2001) Acta Mater 49:265
16. Chen D (1995) Mater Sci Eng A 190:193
17. Wang ZB, Tao NR, Tong WP, Lu J, Lu K (2003) Acta Mater 51:4319
18. Wang ZB, Tao NR, Tong WP, Lu J, Lu K (1996) Defect Diffus Forum 249:147
19. Tong HY, Shi FG, Lavernia EJ (1995) Scripta Metall Mater 32:511
20. Liu L, Li Y, Wang F (2008) Mater Lett 62:4081
21. Zhang XY, Shi MH, Li C, Liu NF, Wei YM (2007) Mater Sci Eng A 448:259
22. Zheng HZ, Lu SQ, Dong XJ, Ouyang DL (2008) Mater Sci Eng A 496:524
23. Niu Y, Cao ZQ, Gesmundo F, Farne G, Randi G, Wang CL (2003) Corros Sci 45:1125
24. Hossain MK (1979) Corros Sci 19:1031
25. Singh Raman RK (1998) Metall Mater Trans A 28A:577
26. Singh Raman RK (1995) Metall Mater Trans A 26A:1847
27. Wood GC (1961) Corros Sci 2:173
28. Giggins CS, Pettit FS (1969) Trans TMS-AIME 245:2509
29. Kofstad P (1988) High temperature corrosion. Elsevier Applied Science & Publishers Ltd., New York
30. Baer RD, Merz MD (1980) Metall Trans 11A:1973
31. Trindade VB, Krupp U, Hanjari BZ, Yang S, Christ H (2005) Mater Res 8:371
32. Keijser THd, Langford JI, Mittemeijer EJ, Vogels ABP (1982) J Appl Crystallogr 15:308
33. Singh Raman RK, Tyagi AK (1994) Mater Sci Eng A 185:97
34. Rees EE, McPhail DS, Ryan MP, Kelly J, Dowsett MG (2003) Appl Surf Sci 203–204:660
35. Ehlers J, Young DJ, Smaardijik EJ, Tyagi AK, Penkalla HJ, Singheiser L, Quadakkers WJ (2006) Corros Sci 48:3428
36. Wagner CJ (1952) Electrochem Soc 99:369; 103:571 (1956)
37. Wagner C (1965) Corros Sci 5:751